Interaction of the Substrate Radical and the 5′-Deoxyadenosine-5′-Methyl Group in Vitamin B_{12} Coenzyme-Dependent Ethanolamine Deaminase

Kurt Warncke* and Andrew S. Utada

Contribution from the Department of Physics, Emory University, Atlanta, Georgia 30322

Received October 12, 2000. Revised Manuscript Received June 22, 2001

Abstract: The distance and relative orientation of the C5′ methyl group of 5′-deoxyadenosine and the substrate radical in vitamin B_{12} coenzyme-dependent ethanolamine deaminase from *Salmonella typhimurium* have been characterized by using X-band two-pulse electron spin−echo envelope modulation (ESEEM) spectroscopy in the disordered solid state. The (*S*)-2-aminopropanol-generated substrate radical catalytic intermediate was prepared by cryotrapping steady-state mixtures of enzyme in which catalytically exchangeable hydrogen sites in the active site had been labeled by previous turnover on $^2H_4$-ethanolamine. Simulation of the time- and frequency-domain ESEEM requires two types of coupled ^2H. The strongly coupled ^2H has an effective dipole distance (r_{eff}) of 2.2 Å, and isotropic coupling constant (A_{iso}) of −0.35 MHz. The weakly coupled ^2H has r_{eff} = 3.8 Å and A_{iso} = 0 MHz. The best ^2H ESEEM time- and frequency-domain simulations are achieved with a model in which the hyperfine couplings arise from one strongly coupled hydrogen site and two equivalent weakly coupled hydrogen sites located on the C5′ methyl group of 5′-deoxyadenosine. This model indicates that the unpaired electron on C1 of the substrate radical and C5′ are separated by 3.2 Å and are thus at closest contact. The close proximity of C1 and C5′ indicates that C5′ of the 5′-deoxyadenosyl moiety directly mediates radical migration between cobalt in cobalamin and the substrate/product site over a distance of 5−7 Å in the active site of ethanolamine deaminase.

Introduction

Homolytic cleavage of the cobalt−carbon bond of adenosylcobalamin (vitamin B_{12} coenzyme, Figure 1) to produce Co^{II} in cobalamin and a 5′-deoxyadenosyl-5′-yl radical species is the primary step of radical-mediated catalysis performed by the family of adenosylcobalamin-dependent enzymes.[1−6] During the subsequent catalytic sequence, hydrogen atom abstraction from the bound substrate generates a substrate radical that is activated for rearrangement to a product radical. A second hydrogen atom transfer then leads to the formation of diamagnetic product, which dissociates from the site. Two types of pathways for the migration of radical character between the β-face of cobalamin and the substrate/product binding site have been proposed,[1−6] as depicted in Figure 2. In Path 1, the 5′-deoxyadenosyl radical ($AdCH_2^{\bullet}$) directly abstracts a hydrogen atom from the substrate, forming 5′-deoxyadenosine and a substrate radical. The 5′-deoxyadenosyl radical is reformed when hydrogen is transferred from the 5′-carbon (C5′) of 5′-deoxyadenosine to the rearranged product radical. In Path 2, the 5′-deoxyadenosyl radical exchanges hydrogen with an intermediate protein-based site ($X^{\bullet}$/XH), which directly interacts with the substrate and product species. In each pathway, the substrate activator radical, $AdCH_2^{\bullet}$ or $X^{\bullet}$, may mediate multiple substrate-to-product conversions before the cobalt−carbon bond is reformed (radical chain length >1; terminal path B in Figure 2), or the intact coenzyme may be reformed following each turnover (radical chain length =1; terminal path A). In the present work we characterize the pathway of radical migration and address the mechanism of hydrogen atom exchanges in the Class II adenosylcobalamin-dependent enzyme, ethanolamine deaminase[1,3,10,11] (also known as ethanolamine-ammonia lyase), which catalyzes the conversion of aminoethanol to ethanal (acetaldehyde) and ammonia.[12]

Evidence for the identity of the participants in the radical migration in B_{12} enzymes was originally gathered from steady-state hydrogen isotope exchange studies and electron paramagnetic resonance (EPR) spectroscopy of trapped radical intermediates.[1,2,5] In ethanolamine deaminase, the exchange of tritium from 1-[^{3}H]-aminoethanol into the coenzyme, and, in separate experiments, the release of tritium from 5′-[^{3}H]-adenosylcobal-

* Corresponding author. Department of Physics, 1001 Rollins Research Center, 1510 Clifton Road, Emory University, Atlanta, GA 30322, Telephone: 404-727-2975. Fax: 404-727-0873. E-mail: kwarncke@physics.emory.edu.

(1) Babior, B. M.; Krouwer, J. S. *CRC Crit. Rev. Biochem*, 35−102, 1979.
(2) *B_{12}*; Dolphin, D., Ed.; Wiley: New York, 1982; Vols. 1 and 2.
(3) Frey, P. *Chem. Rev.* **1990**, *90*, 1343−1357.
(4) Buckel, W.; Golding, B. T. *Chem. Soc. Rev.* **1996**, *25*, 329−338.
(5) Stubbe, J.; van der Donk, W. A. *Chem. Rev.* **1998**, *98*, 705−762.
(6) Banerjee, R. *Chemistry and Biochemistry of B12*; Wiley: New York, 1999.
(7) Glusker, J. P. In *B12*; Dolphin, D., Ed.; Wiley: New York, 1982; Vol. 1, pp 23−107.
(8) Kratky, K.; Kräutler, B. In *Chemistry and Biochemistry of B12*; Banerjee, R., Ed.; Wiley: New York, 1999; pp 9−41.
(9) (a) Ke, S.-C., Torrent, M., Musaev, D. G., Morokuma, K.; Warncke, K. *Biochemistry* **1999**, *38*, 12681−12689. (b) Abend, A.; Bandarian, V.; Nitsche, R.; Stupperich, E.; Retey, J.; Reed, G. H. *Arch. Biochem. Biophys.* **1999**, 370, 138−141.
(10) Babior, B. M. In: *B12*; Dolphin, D., Ed.; Wiley: New York, 1982; Vol. 2, Chapter 10.
(11) Bandarian, V.; Reed, G. H. In *Chemistry and Biochemistry of B12*; Banerjee, R., Ed.; Wiley: New York, 1999; pp 811−833.
(12) Bradbeer, C. *J. Biol. Chem.* **1965** *240*, 4669.

10.1021/ja003658l CCC: $20.00
Published on Web 08/10/2001

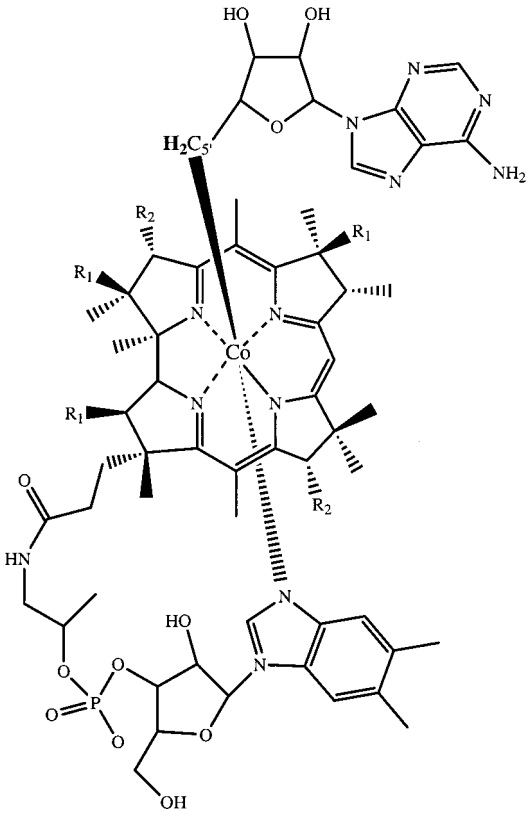

Figure 1. Depiction of the structure of vitamin B_{12} coenzyme [adenosylcob(III)alamin or adenosylcobalamin]. The X-ray crystallographic structures of cobalamins have been reviewed.[7,8] The β-axial ligand is the 5′-deoxyadenosyl group (above page plane) and the α-axial ligand is 5,6-dimethylbenzimidazole (below page plane). The coenzyme retains dimethylbenzimidazole as α-axial ligand when bound in ethanolamine deaminase.[9] R_1 and R_2 refer to acetamide and propionamide side chains. The C5′ carbon of 5′-deoxyadenosyl is labeled, and the two exchangeable hydrogen atoms on the coenzyme are shown in bold.

amin to product ethanal,[13−16] during turnover led to early proposals of a minimal mechanism in which the 5′-deoxyadenosyl moiety interacts directly with substrate and product as depicted in Path 1 of Figure 2.[2] More recently, the exchange of deuterium between an enzyme inactivator and 5′-deoxyadenosine[17] and electron−nuclear double resonance studies have provided additional support for this model.[18] However, the large $^1H/^3H$ isotope effect for transfer of tritium from 5′-[^{3}H]-adenosylcobalamin to product (originally reported[15] as 160, and since revised[11] to 100) was incompatible with the notion[15,19] that the three C5′ methyl hydrogen atoms in 5′-deoxyadenosine, one abstracted from substrate aminoethanol and two from the intact coenzyme, were equivalent with respect to the probability of incorporation into the product ethanal. Comparable results were obtained with the mechanistically similar[3,20] Class II enzyme, diol dehydrase.[21−23] A model was proposed to explain the anomalous ^{3}H isotope effects in ethanolamine deaminase and diol dehydrase, which is a hybrid of Paths 1 and 2.[24] In this model, the primary route of radical migration proceeds along Path 2, with the reformed X• radical capable of multiple turnovers without re-formation of the intact coenzyme (radical chain length >1), but in approximately one out of nine such turnovers, the 5′-deoxyadenosyl radical is re-formed and directly exchanges hydrogen with substrate and product. This minor pathway would be responsible for the slow rate of ^{3}H release to product relative to the rate of turnover. Although the substrate radical[25] and product radical[26] have been directly detected in ethanolamine deaminase by EPR spectroscopy, a candidate for a protein radical has not been observed.

In other adenosylcobalamin-dependent enzymes, the pathway of radical migration is more certain.[5] The Class II adenosylcobalamin-dependent ribonucleotide triphosphate reductase subscribes to Path 2[27] and has a radical chain length of one.[28] The transient X• species in this enzyme[29] has been shown by multifrequency EPR studies of rapid freeze−quench samples to be a cysteine thiyl radical.[30,31] The tritium exchange between enzyme-bound 5′-[^{3}H]-adenosylcobalamin and solvent water, which is catalyzed by native effector-activated or catalytically active holoenzyme,[5] can be taken as a signature of the involvement of a heteroatomic protein radical center in radical migration. In contrast to ribonucleotide triphosphate reductase, the Class I carbon skeleton-rearranging enzymes,[4] methylmalonyl-CoA mutase[32] and glutamate mutase,[33] appear to operate by Path 1 of Figure 2. These enzymes do not conduct ^{3}H exchange between the 5′-[^{3}H]-coenzyme and the solvent.[34,35] In addition, the rate of cobalt−carbon bond cleavage is slowed by substitution of deuterium for hydrogen at the position of hydrogen atom exchange on the substrate or product.[36,37] These results have been interpreted in terms of the direct exchange of hydrogen between the 5′-deoxyadenosyl moiety and substrate and product in the glutamate and methylmalonyl-CoA mutases.[36,37]

(13) Babior, B. M. *Biochim. Biophys. Acta* **1968**, 167, 456−458.
(14) Carty, T. J.; Babior, B. M.; Abeles, R. H. *J. Biol. Chem.* **1971**, *246*, 6313−6317.
(15) Weisblat, D. A.; Babior, B. M. *J. Biol. Chem.* **1971**, *246*, 6064−6071.
(16) Carty, T. J.; Babior, B. M.; Abeles, R. H. *J. Biol. Chem.* **1974** *249*, 1683−1688.
(17) Bandarian, V., Poyner, Russel R.; Reed, G. H. *Biochemistry* **1999**, *38*, 12403−12407.
(18) A pulsed-electron−nuclear double resonance (ENDOR) study of the substrate radical state appeared while the present report was under revision: LoBrutto, R.; Bandarian, V.; Magnusson, O. Th.; Chen, X.; Schramm, V. L.; Reed, G. H. *Biochemistry* **2001**, *40*, 9−14.
(19) Babior, B. M. *J. Biol. Chem.* **1969** *244*, 449.
(20) Toraya, T. In *Chemistry and Biochemistry of B12*; Banerjee, R., Ed.; Wiley: New York, 1999; pp 783−810.
(21) Frey, P. A.; Kerwar, S. S.; Abeles, R. H. *Biochem. Biophys. Res. Comm.* **1967**, *29*, 873−879.
(22) Frey, P. A.; Essenberg, M. K.; Abeles, R. H. *J. Biol. Chem.* **1967**, *242*, 5369−5377.
(23) Essenberg, M. K.; Frey, P. A.; Abeles, R. H. *J. Am. Chem. Soc.* **1971**, *93*, 1242−1251.
(24) Cleland, W. W. *CRC Crit. Rev. Biochem.* **1982**, *13*, 385−428.
(25) Babior, B. M.; Moss, T. H.; Orme-Johnson, W. H.; Beinert, H. *J. Biol. Chem.* **1974** *249*, 4537−4544.
(26) Warncke, K.; Schmidt, J. C.; Ke, S.-C. *J. Am. Chem. Soc.* **1999**, *121*, 10522−10528.
(27) Booker, S.; Licht, S.; Broderick, J.; Stubbe, J. *Biochemistry* **1994**, *33*, 12676−12685.
(28) Licht, S. S.; Booker, S.; Stubbe, J. *Biochemistry* **1999**, *38*, 1221−1233.
(29) Orme-Johnson, W. H.; Beinert, H.; Blakley, R. L. *J. Biol. Chem.* **1974**, *249*, 2338−2343.
(30) Licht, S.; Gerfen, G. J.; Stubbe, J. *Science* **1996**, *271*, 477−481.
(31) Gerfen, G. J.; Licht, S.; Willems, J.-P.; Hoffman, B. M.; Stubbe, J. *J. Am. Chem. Soc.* **1996**, *118*, 8192−8197.
(32) Banerjee, R.; Chowdhury, S. In *Chemistry and Biochemistry of B12*; Banerjee, R., Ed.; Wiley: New York, 1999; pp 707−730.
(33) Buckel, W.; Bröker, G.; Bothe, H.; Pierik, A. J.; Golding, B. T. In *Chemistry and Biochemistry of B12*; Banerjee, R., Ed.; Wiley: New York, 1999; pp 757−782.
(34) Marsh, E. N. G. *Biochemistry* **1995**, *34*, 7542−7547.
(35) Meier, T. W.; Thöma, N. H.; Leadley, P. F. *Biochemistry* **1996**, *35*, 11791−11796.
(36) Padmakumar, R.; Padmakumar, R.; Banerjee, R. *Biochemistry* **1997**, *36*, 3713−3718.
(37) Marsh, E. N. G.; Ballou, D. P. *Biochemistry* **1998**, *37*, 11864−11872.

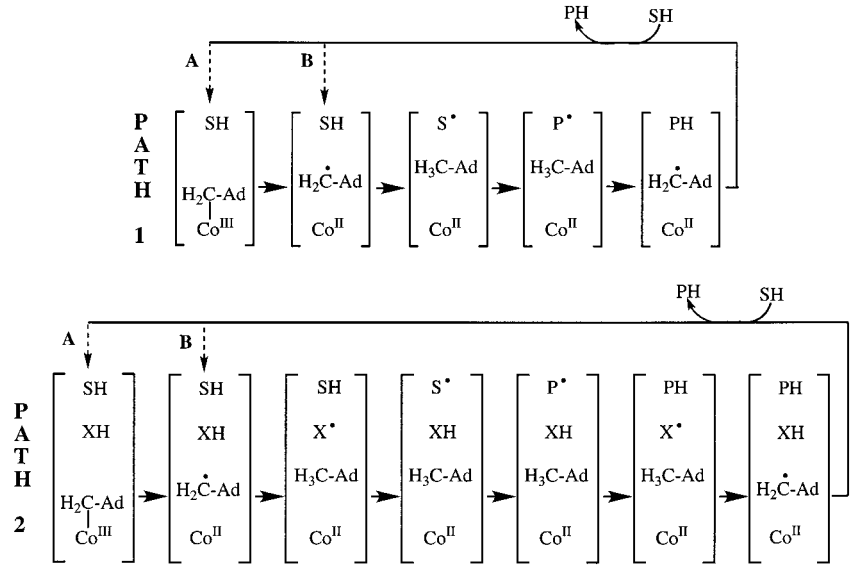

Figure 2. Pathways of radical migration in vitamin B_{12} coenzyme-dependent enzymes.[3,4,5] The forward direction of reaction is indicated by arrows. In ethanolamine deaminase, the detectable reversibility of individual steps varies among the different substrates.[10] Substrate-derived species in the radical pair states are designated S−H (bound substrate), S• (substrate radical), P• (product radical) and PH (bound products). The 5′-deoxyadenosyl β-axial ligand is represented as Ad-CH_2- in the intact coenzyme, and as Ad-CH_2• (5′-deoxyadenosyl radical) or Ad-CH_3 (5′-deoxyadenosine) following cobalt−carbon bond cleavage. In Path 2, X•/XH represents an intermediate protein-based, hydrogen atom transfer couple. The cobalt ion and its formal oxidation states are depicted, but the corrin ring and α-axial ligand of the coenzyme are not shown for clarity. Details of Paths 1A, 1B, 2A and 2B are described in the text.

To gain insight into the participation of the 5′-deoxyadenosyl moiety and any other hydrogen exchange centers in the radical migration in ethanolamine deaminase from *Salmonella typhimurium* we have addressed the relative active-site position of hydrogen exchange sites during catalysis by measuring the magnetic interactions of the unpaired electron spin at C1 of the substrate radical with the nuclear spins of ^{2}H incorporated into hydrogen exchange sites by reaction with 1,1,2,2-$^2H_4$-aminoethanol. The substrate radical accumulates during steady-state turnover on the non-native substrate, 2-aminopropanol,[25] and is stabilized for electron paramagnetic resonance spectroscopic investigations by cryotrapping.[25,38] The electron spin−echo envelope modulation (ESEEM) technique of pulsed-EPR spectroscopy has been chosen to measure the electron−^{2}H hyperfine couplings.[39−41] This is because the presence of the electron spin and deuteron spins on separate molecules is likely to lead to weak hyperfine coupling. It is not possible to resolve weak hyperfine splittings in the substrate radical EPR line shape, because of inhomogeneous broadening in the disordered solid-state samples,[25,38] whereas ESEEM spectroscopy has proven successful in investigations of weak couplings.[9,38,42] A second advantage of ESEEM spectroscopy is that the modulation amplitude (envelope modulation depth) corresponds directly to the number of coupled nuclei.[43,44] This is important for the present studies, where multiple distinct ^{2}H hyperfine couplings contribute to the modulation. The relative modulation contributions, and thus relative hydrogen site occupancies, can be determined for different classes of coupled ^{2}H nuclei.

ESEEM simulation analysis of experimental multifrequency X-band ESEEM resolves the hyperfine tensors and relative modulation contributions of two distinct types of deuterons that are coupled to the unpaired electron spin localized at C1 of the substrate radical. Using an explicit model for the interactions, the coupled ^{2}H are assigned to the three methyl hydrogen positions on C5′ of 5′-deoxyadenosine. The model fixes the positions of the C5′ hydrogen nuclei relative to C1 and indicates that C1 and C5′ are at closest contact. The close proximity of the C1 and C5′ centers indicates that the 5′-deoxyadenosyl moiety exchanges hydrogen directly with the substrate and product species.

Experimental Procedures

Enzyme Preparation. Enzyme was purified from the *Eschericia coli* overexpression strain incorporating the cloned *S. typhimurium* ethanolamine deaminase coding sequences[45] essentially as described,[46] with the exception that the enzyme was dialyzed against buffer containing 100 mM HEPES (pH 7.45), 10 mM KCl, 5 mM dithiothreitol, 10 mM urea, and 10% glycerol.[47] Enzyme activity was determined as described[48] by using the coupled assay with alcohol dehydrogenase/NADH. The specific activity of the purified enzyme with aminoethanol as substrate was 20−25 μmol/min/mg.

Sample Preparation. Adenosylcobalamin (Sigma Chemical Co.), natural abundance aminoethanol, 1,1,2,2-$^2H_4$-aminoethanol (Cambridge Isotope Laboratories, Inc.) and (*S*)-2-aminopropanol (Aldrich Chemical Co.) were purchased from commercial sources. The reactions were performed in air-saturated buffer containing 100 mM HEPES (pH 7.5), 10 mM KCl, and 5 mM dithiothreitol. Identical results were obtained with air-saturated and anaerobic samples. All manipulations were carried out under red safe-lighting.

(38) Ke, S.-C.; Warncke, K. *J. Am. Chem. Soc.* **1999**, *121*, 9922−9927.
(39) Kevan, L.; Bowman, M. K. *Modern Pulsed and Continuous Wave Electron Spin Resonance*; Wiley: New York, 1990.
(40) Schweiger, A. *Angew. Chem., Int. Ed. Engl.* **1991**, *30*, 265.
(41) Dikanov, S. A.; Tsvetkov, Yu. D. *Electron Spin−Echo Envelope Modulation Spectroscopy*; Chemical Rubber, Boca Raton, Florida, 1993.
(42) Tan, S. L.; Kopczynski, M. G.; Bachovchin, W. W.; Orme-Johnson, W. H.; Babior, B. M. *J. Biol. Chem.* **1986** *261*, 3483−3485.
(43) Rowan, L. G.; Hahn, E. L.; Mims, W. B. *Phys. Rev.* **1965**, *137*, A61-A67.
(44) Mims, W. B. *Phys. Rev. B* **1972**, *5*, 2409−2419.
(45) Faust, L. P.; Connor, J. A.; Roof, D. M.; Hoch, J. A.; Babior, B. M. *J. Biol. Chem.* **1990**, *265*, 12462−12466.
(46) Faust, L. P.; Babior, B. M. *Arch. Biochem. Biophys.* **1992**, *294*, 50−54.
(47) Harkins, T. T.; Grissom, C. B. *J. Am. Chem. Soc.* **1995**, *117*, 566−567.
(48) Kaplan, B. H.; Stadtman, E. R. *J. Biol. Chem.* **1968**, *243*, 1787−1793.

The substrate radical was generated by using a procedure for fast cryotrapping of steady-state intermediate states in ethanolamine deaminase.[26] All manipulations were carried out on ice in a cold room. The final concentration of enzyme was 30 mg/mL, which is equivalent to 60 μM for a holoenzyme molecular mass of 500,000 g/mol. Adenosylcobalamin was added to 360 μM, which is stoichiometric with active sites. The active-site/holoenzyme stoichiometry of 6 is based on adenosylcobalamin titrations of substrate radical formation (K. Warncke, unpublished) and is in agreement with the value obtained by two different methods.[49,50] Other determinations have yielded active site/holoenzyme values of 2.[46,51] The source of the discrepancy in active site/holoenzyme values is unclear but does not influence the conclusions drawn from the present work.

In the ^{2}H-prelabeling reactions with $^2H_4$-aminoethanol, and parallel control reactions with natural abundance aminoethanol, reaction was initiated by addition of adenosylcobalamin to premixed enzyme and 36 mM aminoethanol. The reaction with aminoethanol was allowed to proceed for 2 min. After reaction for 2 min, no EPR signal is detected from the product radical intermediate that is present at earlier incubation times.[26] The disappearance of the product radical signal indicates that the conversion of substrate to product has proceeded to completion, in agreement with the reaction extent calculated from the turnover number.[26,52] After the 2 min incubation with aminoethanol, 10 mM 2-aminopropanol was added, and after an additional 12−15 s time interval, during which the sample was loaded into a 4 mm o.d. EPR tube, the sample was plunged into liquid nitrogen-chilled isopentane ($T \approx 130$ K) to freeze.

We assume that the ^{2}H-prelabeling treatment with $^2H_4$-aminoethanol has gone to completion and, therefore, that all catalytically relevant hydrogen exchange sites are occupied by ^{2}H. This assumption is supported by studies of the dependence of the ^{2}H ESEEM amplitude on the number of turnovers on $^2H_4$-aminoethanol during pretreatment, in which the amplitude was shown to be saturated at the level of 100 $^2H_4$-aminoethanol/active site used in the present studies (J. M. Canfield and K. Warncke, in preparation). The large ^{1}H/^{2}H isotope effects for the second hydrogen atom transfer step,[10] and direct chemical analysis of complete ^{2}H incorporation into C5′ of deoxyadenosine after several turnovers on deuterated substrates and inhibitors,[17] also support the assumption of full ^{2}H incorporation.

Continuous-Wave EPR Spectroscopy. CW-EPR spectra were obtained by using a Bruker ER200D EPR spectrometer equipped with a Bruker 4102ST TE102 cavity, HP 4256L frequency counter, Varian V3603 electromagnet and VFR2503 regulator/power supply, and Varian cryostat assembly with Air Products temperature controller for nitrogen gas flow sample cooling.

ESEEM Spectroscopy. Data Acquisition and Processing. ESEEM was collected by using the two-pulse microwave pulse sequence[39−41] on a home-constructed wideband pulsed-EPR spectrometer that will be described elsewhere (K. Warncke, in preparation). Envelope modulation was deadtime-reconstructed[53] and cosine Fourier transformed to generate ESEEM frequency spectra. All data processing and analysis were performed with routines written in Matlab (Mathworks, Natick, MA) script and run on PowerMacintosh or PC computers.

ESEEM Simulations. Computational Approach. The coupled electron−nuclear spin system of the radical was described by the following stationary-state Hamiltonian:

$$H = \beta_e \mathbf{S} \bullet \mathbf{g_e} \bullet \mathbf{B_0} + h\mathbf{S} \bullet \mathbf{A} \bullet \mathbf{I} - g_n \beta_n \mathbf{B_0} \bullet \mathbf{I} + \mathbf{I}' \bullet \mathbf{Q} \bullet \mathbf{I}' \qquad (1)$$

where g_e, β_e, and g_n, β_n are the electron and nuclear g-value and magneton, respectively, $\mathbf{g_e}$ is the electron **g**-tensor, $\mathbf{B_0}$ is the external magnetic field vector, h is Planck's constant, **A** is the hyperfine interaction tensor, **Q** is the nuclear quadrupole interaction tensor, and the **S** and **I** are electron and nuclear spin operators. In the strong field approximation assumed here, the electron Zeeman interaction is given by $g_e\beta_e\mathbf{B_0}S_z'$, where S_z' is the fictitious spin operator.[54,55] The pulse time-domain ESEEM was simulated by direct implementation of the density matrix formalism of Mims.[44,56] Details of the simulation analysis procedures, and justification for the application of the Hamiltonian in eq 1 to the radical in the weakly coupled Co^{II}−substrate radical pair state in ethanolamine deaminase, have been described.[9,38] The simulated ESEEM incorporated the same deadtime as the data, and it was deadtime-reconstructed and processed in exactly the same way as the experimental ESEEM. ESEEM simulations were performed with routines written in Matlab (Mathworks, Natick, MA) script and run on PowerMacintosh or PC computers.

Adjustable and Fixed Simulation Parameters. In the ESEEM simulations, the variable input parameters include the following: The diagonal hyperfine tensor, $[A_{xx}, A_{yy}, A_{zz}]$, which is the sum of an isotropic component (A_{iso}) and an axially symmetric dipolar tensor, $[-A_{dip}, -A_{dip}, 2A_{dip}]$, where $A_{dip} = g_e\beta_e g_n\beta_n h^{-1} r_{eff}^{-3}$ (MHz) and r_{eff} is the effective distance separating the unpaired electron and nuclear spins. The single parameter, r_{eff}, thus determines the dipolar tensor. For ^{2}H coupling, nuclear quadrupole interaction parameters represent the magnitude of the interaction (quadrupole coupling constant, e^2qQ/h), the asymmetry of the electric field gradient (asymmetry parameter, η), and Euler angles, $[\alpha, \beta, \gamma]$, which define the mutual orientation of the nuclear quadrupole and hyperfine tensor principal axes. The free electron and nuclear frequencies are fixed by the experimental magnetic field value. A compendium of ^{2}H nuclear quadrupole coupling parameters[57] shows that the e^2qQ/h and η values for ^{2}H bonded to carbon are comparable, with typical values of 0.12 MHz and 0.0−0.1, respectively. Therefore, fixed $e^2qQ/h = 0.12$ MHz and $\eta = 0.1$ were used. The Euler angles relating the nuclear quadrupole and hyperfine tensors were fixed at $\alpha = \beta = \gamma = 0°$, corresponding to the case of coincident hyperfine and nuclear quadrupole interaction principal axes. Variation of the angle β did not significantly influence the simulations.

The variable parameters were adjusted, and the best match of the simulated and experimental time and frequency domain data was determined by visual scrutiny of overlaid data and simulations. The limits on the parameter values represent values that, if exceeded, led to significantly poorer reproduction of the experimental data.

Combination of ESEEM from Multiple Hyperfine Couplings. When N nuclear spins are coupled to the same unpaired electron spin, the two-pulse ESEEM is given by the product of the ESEEM from the N individual hyperfine couplings, as follows:[43,56]

$$E_{T,mod}(\tau) = \prod_i^N E_{mod,i}(\tau) \qquad (2)$$

Here, $E_{T,mod}(\tau)$ is the τ-dependent total envelope modulation, and $E_{mod,i}(\tau)$ is the envelope modulation function for coupled nucleus i. Spherical averaging is performed for the ESEEM from each hyperfine coupling prior to taking the product in eq 2.[58,59]

The treatment of multiple hyperfine coupling contributions to ESEEM in systems with partial isotope occupancy of a single nuclear site has been described.[43] A general expression for two-pulse ESEEM for hydrogen isotopes that exhibit partial occupancy at multiple nuclear (hydrogen) sites is given by:

(49) Hollaway, M. R.; Johnson, A. W.; Lappert, M. F.; Wallis, O. C. *Eur. J. Biochem.* **1980**, *111*, 177−188.
(50) Bandarian, V.; Reed, G. H. *Biochemistry* **1999**, *38*, 12394−12402.
(51) (a) Babior, B. M. *J. Biol. Chem.* **1969**, *244*, 2927−2934. (b) Babior, B. M.; Li, T. K. *Biochemistry* **1969**, *8*, 154−160.
(52) Babior, B. M.; Gould, D. C. *Biochem. Biophys. Res. Commun.* **1969**, *34*, 441−447.
(53) Mims, W. B. *J. Magn. Reson.* **1984**, *59*, 291−306.
(54) Abragam, A.; Bleaney, B. *Electron Paramagnetic Resonance of Transition Ions*; Dover: New York, 1986; pp 133−178.
(55) Hutchison, C. A.; McKay, D. B. *J. Chem. Phys.* **1977**, *66*, 3311.
(56) Mims, W. B. *Phys. Rev. B* **1972**, *6*, 3543.
(57) *Landolt-Börnstein Numerical Data and Functional Relationships in Science and Technology*; Hellwege, K.-H., Hellwege, A. M., Eds.; Springer-Verlag: New York, 1988; Subvol. a.
(58) Mims, W. B.; Davis, J. L.; Peisach, J. *J. Magn. Reson.* **1990**, *86*, 273−292.
(59) Kevan, L. In *Time Domain Electron Spin Resonance*; Kevan, L., Bowman, M. K., Eds.; Wiley: New York, 1979; pp 279−342.

$$E_{\mathrm{T,mod}} = \{ \sum_{j}^{M} F_j [\prod_{i}^{N} E_{\mathrm{mod},i}(^{x}\mathrm{H})] \} \prod_{k}^{P} E_{\mathrm{mod},k} \qquad (3)$$

The τ descriptor is not included for clarity in eq 3 and subsequent equations. As in eq 2, "*i*" indexes one of the *N* distinct nuclear sites, which can be occupied by protium ($x = 1$; natural abundance) or deuterium ($x = 2$; specifically incorporated). The contributions of *P* other hyperfine couplings are included in the product over *k*. Depending on the value of *N* and the level of ^{2}H replacement of ^{1}H, there will be *j* different populations of active sites, with a maximum possible value of $M = 2^N$. F_j gives the normalized probability ($\Sigma F_j = 1$) of each type of active site in the sample. Each type of active site contributes additively to the total modulation.

Two models are considered for the combination of the two-pulse ESEEM from the catalytically exchangeable hydrogen hyperfine couplings for the substrate radical in ethanolamine deaminase. In the first model, which is shown schematically in Figure 7A, it is assumed that each unpaired electron spin interacts with two hydrogen sites, which are occupied by ^{2}H nuclei, and eq 3 for the ^{2}H-prelabeled sample becomes:

$$E_{\mathrm{T,mod}} = \{E_{\mathrm{mod},11}(^2\mathrm{H}) E_{\mathrm{mod},12}(^2\mathrm{H})\} \prod_{k}^{P} E_{\mathrm{mod},k} \qquad (4)$$

In the second model, which is shown schematically in Figure 7B, there are three active-site populations ($M = 3$), corresponding to the three hydrogen sites on C5′ of deoxyadenosine, two that are occupied by ^{2}H, and one that is occupied by the ^{1}H abstracted from C1. Equation 3 for the ^{2}H-prelabeled sample becomes:

$$E_{\mathrm{T,mod}} = \{F_1[E(^2\mathrm{H})_{\mathrm{mod},11} E(^2\mathrm{H})_{\mathrm{mod},12} E(^1\mathrm{H})_{\mathrm{mod},13}] + F_2[E(^1\mathrm{H})_{\mathrm{mod},21} E(^2\mathrm{H})_{\mathrm{mod},22} E(^2\mathrm{H})_{\mathrm{mod},23}] + F_3[E(^2\mathrm{H})_{\mathrm{mod},31} E(^1\mathrm{H})_{\mathrm{mod},32} E(^2\mathrm{H})_{\mathrm{mod},33}]\} \prod_{k}^{P} E_{\mathrm{mod},k} \qquad (5)$$

Envelope Division of the Combination ESEEM. Modulation from nuclei other than the catalytically incorporated ^{2}H can be eliminated by dividing the modulation collected for the ^{2}H-labeled sample by the modulation collected for an unlabeled (natural isotopic abundance; assumed here to be all-^{1}H because of the low natural abundance of ^{2}H) sample prepared under identical conditions.[60] The following quotient ESEEM expression for the model of the unpaired electron coupled to two distinct ^{2}H is obtained from eq 4:

$$E_{\mathrm{QT,mod}} = \{E_{\mathrm{mod},11}(^2\mathrm{H})\, E_{\mathrm{mod},12}(^2\mathrm{H})\}/\{E_{\mathrm{mod},11}(^1\mathrm{H}) E_{\mathrm{mod},12}(^1\mathrm{H})\} \qquad (6)$$

The following quotient ESEEM expression for the explicit C5′ methyl group three hydrogen site model is obtained from eq 5:

$$E_{\mathrm{QT,mod}} = F_1[\, E(^2\mathrm{H})_{\mathrm{mod},11}\, E(^2\mathrm{H})_{\mathrm{mod},12}/E(^1\mathrm{H})_{\mathrm{mod},11}\, E(^1\mathrm{H})_{\mathrm{mod},12}] + F_2\,[E(^2\mathrm{H})_{\mathrm{mod},22}\, E(^2\mathrm{H})_{\mathrm{mod},23}/E(^1\mathrm{H})_{\mathrm{mod},22}\, E(^1\mathrm{H})_{\mathrm{mod},23}] + F_3\,[E(^2\mathrm{H})_{\mathrm{mod},31}\, E(^2\mathrm{H})_{\mathrm{mod},33}/\, E(^1\mathrm{H})_{\mathrm{mod},31}\, E(^1\mathrm{H})_{\mathrm{mod},33}\,] \qquad (7)$$

In eq 7, $F_1 = F_2 = F_3 = 0.33$, if there is no equilibrium ^{2}H/^{1}H isotope effect on the occupancies. Equations 6 and 7 show that the contributions of the P coupled nuclei other than the ^{2}H and ^{1}H involved in catalytic exchange are eliminated in the quotient ESEEM.

In practice, the ^{1}H line widths are greater than the corresponding ^{2}H line widths by a factor of 6.51, which is the ratio of the nuclear gyromagnetic ratios for ^{1}H and ^{2}H. Therefore, the bulk of the ^{1}H modulation decays within the deadtime of the pulsed-EPR spectrometer,[61] and the modulation from ^{1}H does not typically make a strong contribution to the quotient ESEEM.

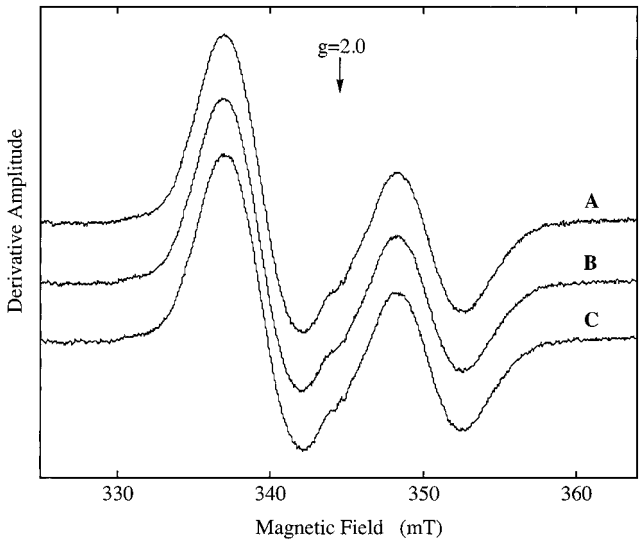

Figure 3. X-band continuous-wave EPR spectra of the substrate radical in ethanolamine deaminase, generated by using (*S*)-2-aminopropanol following different enzyme pretreatments. The free electron resonance position at the *g*-value of 2.00 is shown by the arrow. A low level of an uncharacterized radical is present at $g = 2.0$. (A) No pretreatment; (B) pretreatment with natural abundance, $^1H_4$-aminoethanol; (C) pretreatment with $^2H_4$-aminoethanol. *Conditions*: microwave power, 0.2 mW; microwave frequency, 9.653 GHz; magnetic field modulation, 1.0 mT; modulation frequency, 100 kHz; temperature, 70 K; scan rate, 0.2 mT/s; time constant, 0.2 s; average of four scans minus baseline.

Results

EPR Spectroscopy. Figure 3 shows X-band continuous-wave EPR spectra of the 2-aminopropanol-1-yl substrate radical intermediate in ethanolamine deaminase, obtained by cryotrapping the holoenzyme 15 s after mixing with excess (*S*)-2-aminopropanol substrate. The characteristic doublet line shape[25] in the $g = 2.0$ region arises from exchange and dipolar interactions between the unpaired electron spins localized on the substrate radical and Co^{II} in cobalamin.[62] The amplitude of the broad resonance arising from Co^{II} is most prominent in the *g*(perpendicular) region at $g \approx 2.2$ (here, at ~290 mT)[25] and is therefore not visible in Figure 3.

Figure 3 shows the substrate radical EPR spectrum from enzyme that had not been pretreated with aminoethanol (spectrum A) and from enzyme that was pretreated with natural abundance aminoethanol (spectrum B). These spectra show that pretreatment of the enzyme with natural abundance aminoethanol does not alter the line shape or amplitude of the substrate radical EPR spectrum, relative to the untreated control. This result shows that the integrity of the enzyme and active site is maintained following the aminoethanol pretreatment, since electron spin−spin interactions between the radical and Co^{II} depend on distance and orientation,[62] and changes in these parameters would alter the EPR spectrum. Figure 3C shows that the line shape and amplitude of the substrate radical spectrum are also not altered by pretreatment with $^2H_4$-aminoethanol. Incorporation of ^{2}H for ^{1}H at a site that participates in a strong hydrogen hyperfine interaction with the unpaired spin would result in a narrowing of the line shape, because of the reduction

(60) Mims, W. B.; Peisach, J. In *Advanced EPR: Applications in Biology and Chemistry*; Hoff, A. J., Ed.; Elsevier: New York, 1996; pp 1−57.

(61) Astashkin, A. V.; Dikanov, S. A.; Tsvetkov, Yu. D. *Chem Phys Lett* **1987**, *136*, 204−208.

(62) Boas, J. F.; Hicks, P. R.; Pilbrow, J. R. *J. Chem. Soc. Faraday II* **1978**, *74*, 417−431.

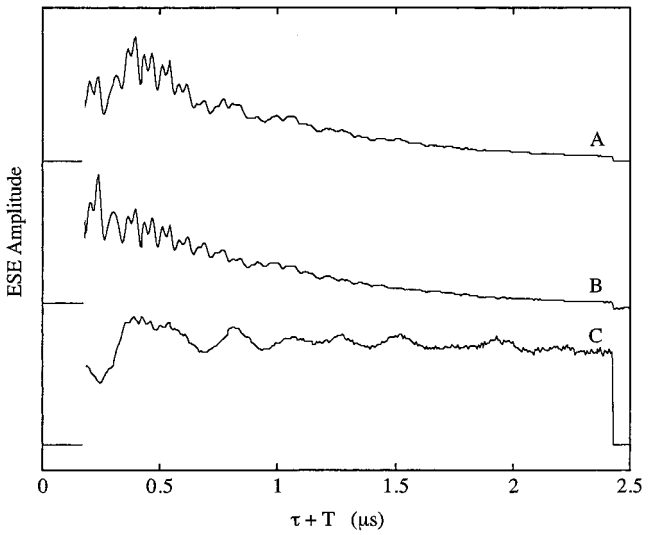

Figure 4. Experimental two-pulse ESEEM collected from the (*S*)-2-aminopropanol-generated substrate radical in ethanolamine deaminase. The vertical axis corresponds to the integrated area of the electron spin−echo. Each waveform is individually normalized so that the maximum−minimum amplitude is the same for all. (A) ESEEM from enzyme pretreated with $^2H_4$-aminoethanol. (B) ESEEM from enzyme pretreated with natural abundance ($^1H_4$-) aminoethanol. (C) Quotient ESEEM, obtained by dividing the ESEEM in (A) by ESEEM in (B). *Conditions*: temperature, 6 K; magnetic field, 310.5 mT; microwave frequency, 8.83 GHz (*g*-value, 2.03); microwave pulse power, 40 W; initial τ value, 176 ns; τ increment, 6 ns; $\pi/2$ pulse width, 20 ns; pulse repetition rate, 64 Hz; 100 repetitions averaged per point; average of 4 envelopes.

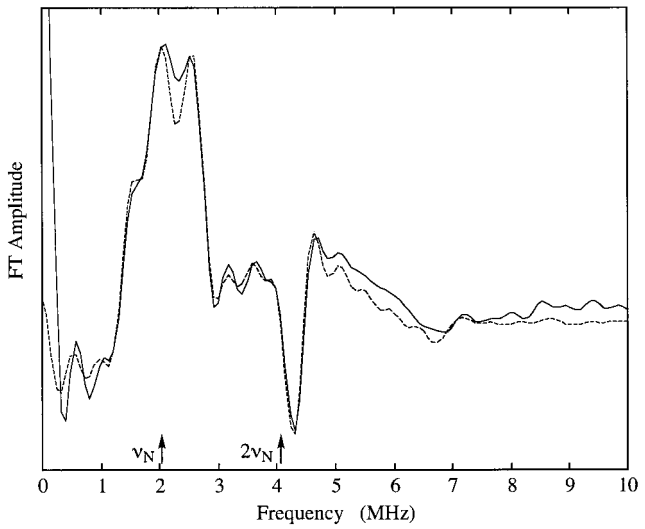

Figure 5. Experimental two-pulse quotient ESEEM frequency spectrum (solid line) for the (*S*)-2-aminopropanol-generated substrate radical in ethanolamine deaminase and overlaid quotient ESEEM simulation (dashed line). The experimental spectrum is the cosine Fourier transform of the quotient waveform shown in Figure 4C. The arrows mark the positions of the free deuteron resonance frequency (ν_N) and twice this frequency ($2\nu_N$). Experimental data collection conditions are described in the legend to Figure 4. The simulated spectrum is the Fourier transform of the envelope modulation shown in Figure 8B.

in nuclear gyromagnetic ratio, by a factor of 6.51 for ^2H relative to ^1H.[63] A reduction in line width accompanies specific ^2H-substitution at C1 of the substrate radical, whereas ^2H substitution at C2 has no effect.[25] Therefore, the α-^1H nuclei at C1, or any other ^1H nuclei that are strongly coupled to the unpaired electron spin, are not significantly exchanged.

ESEEM Spectroscopy. Identification of Substrate Radical-^2H Hyperfine Coupling. Figure 4 shows the time-domain two-pulse ESEEM collected for the (*S*)-2-aminopropanol-generated substrate radical in enzyme pretreated with $^2H_4$- and $^1H_4$-aminoethanol. In the ESEEM experiment, the modulation of the echo envelope occurs with a periodicity corresponding to the hyperfine and nuclear quadrupole (for $I \geq 1$) frequencies of nuclear spins that are coupled to the unpaired electron spin.[43,44] The waveform in Figure 4B for the $^1H_4$-aminoethanol pretreated enzyme shows a short-period modulation (76 ns; $\nu_{max} = 13.2$ MHz) that arises from the multitude of matrix ^1H nuclei in the protein and solvent surrounding the radical, which are coupled to the unpaired spin through weak dipolar interactions. The longer-period modulation components arise from coupling to a ^{14}N nucleus located in the active site.[38,42] The envelope modulation for the $^2H_4$-aminoethanol-pretreated enzyme, displayed in Figure 4A, shows additional modulation components superposed on the ^1H and ^{14}N modulation. The ^2H envelope modulation components can be separated from the ^1H and ^{14}N modulation common to each radical by dividing the envelope modulation in Figure 4A by the modulation in Figure 4B.[60] The resulting quotient modulation, presented in Figure 4C, is dominated by a component with a period of approximately 500 ns, which is the reciprocal of the free deuteron frequency (2.04 MHz) at the applied magnetic field of 310.5 mT. These results indicate that the 2-aminopropanol-generated substrate radical interacts with ^2H nuclei incorporated into the holoenzyme complex by the $^2H_4$-aminoethanol pretreatment.

Characterization of the ^2H ESEEM. Quotient envelope modulation collected for the substrate radical generated from (*S*)-2-aminopropanol, shown in Figure 4, was Fourier transformed to obtain the corresponding ESEEM frequency spectrum displayed in Figure 5. The spectrum shows a line shape centered about the free ^2H frequency. The relatively weak ^2H hyperfine splitting of <0.07 mT is consistent with the lack of an effect of $^2H_4$-aminoethanol-prelabeling on the EPR line shapes, as shown in Figure 3.

The ^2H ESEEM line shape shown in Figure 5 is composed of the following four principal features: (1) A narrow line is centered around the free ^2H frequency (maximum amplitude, 2.09 MHz) and is suggestive of one or more relatively weakly coupled deuterons. (2) The narrow line shape component overlaps a broad feature, also centered around 2.0 MHz. The broad feature shows greater amplitude on the high-frequency side of the free ^2H frequency, with a resolved peak at 2.52 MHz. A shoulder on the low-frequency side is positioned at 1.54 MHz. The peak and shoulder are symmetrically split about the free ^2H frequency, suggesting that they correspond to the α ($m_s = +1/2$)- and β ($m_s = -1/2$)-manifold features of the same hyperfine coupling. (3) An intense [$\nu_\alpha + \nu_\beta$] sum combination line,[43,64] distinguished by a negative phase, is centered at 4.31 MHz. The splitting of the sum combination line from the position corresponding to twice the free ^2H nuclear frequency ($2\nu_N = 4.08$ MHz at 310.5 mT) is diagnostic of the strength of the dipolar hyperfine coupling.[64] The splitting of 0.23 MHz shows that one of the ^2H hyperfine couplings that gives rise to the fundamental features around 2.0 MHz has a relatively strong (short range) dipolar coupling component. (4) A feature that

(63) Wertz, J. E.; Bolton, J. R. *Electron Spin Resonance*; Chapman & Hall, New York, 1986.

(64) Astashkin, A. V.; Dikanov, S. A. In *Advanced EPR: Applications in Biology and Chemistry*; Hoff, A. J., Ed.; Elsevier: New York, 1996; pp 59−117.

arises predominantly from the $\Delta m_I = \pm 2$ frequencies for the ^{2}H hyperfine couplings gives broad intensity that extends from the high-frequency side of the fundamental features up to approximately 6.0 MHz. Multifrequency ESEEM performed at 10.3 and 10.9 GHz confirms the ^{2}H origin of the features and the absence of significant contributions from other nuclear couplings in the ^{2}H region.

In addition to the ^{2}H features shown in Figure 5, features from the ^{1}H replaced by the ^{2}H nuclei are observed at and near the position of the ^{1}H [$\nu_\alpha + \nu_\beta$] sum combination line (data not shown). These features are being further studied by using high-resolution four-pulse ESEEM experiments. In contrast to the typically narrow (and therefore observable) ^{1}H sum combination features,[43,64] the fundamental ^{1}H features are not clearly resolved. In addition to overlap with the strong ^{2}H features, the ^{1}H fundamental features have a 6.51-fold greater line width than the corresponding ^{2}H features, which indicates that most of the intensity decays within the deadtime of the pulsed-EPR spectrometer.

Discussion

Simulation of the ^{2}H ESEEM Envelope Modulation and Line shapes. ^{2}H Hyperfine Coupling Parameters. Simulation of the experimental ESEEM required a relatively strong ^{2}H dipolar hyperfine coupling. The position of the hydrogen [$\nu_\alpha + \nu_\beta$] sum combination line is very sensitive to the electron−nuclear distance at short separations[64] and therefore provided the key constraint on the value of r_{eff} for the strongly coupled deuteron. A ^{2}H dipolar coupling with $r_{eff} = 2.2$ Å reproduced the frequency position of 4.31 MHz and the amplitude of the sum combination feature. As an example of the sensitivity of the sum combination line to r_{eff}, values of 2.1 and 2.3 Å gave sum combination lines positioned at 4.38 and 4.23 MHz, respectively. The uncertainty in the value of r_{eff} is thus less than 0.1 Å. An ESEEM spectrum simulated from the all-dipolar, $r_{eff} = 2.2$ Å coupling produced broad intensity in the fundamental region around 2.0 MHz. However, the low-frequency shoulder and high-frequency peak positions were insufficiently split from the free ^{2}H frequency to match the experimental line shape. Introduction of an isotropic hyperfine coupling constant of −0.35 MHz led to correct low-frequency shoulder and high-frequency peak placement, while maintaining the match to the sum combination line. Values of $A_{iso} > 0$ gave unsatisfactory simulations. The effect of the negative isotropic coupling on the fundamental feature is to move the $m_s = +^1/_2$ and $m_s = -^1/_2$ perpendicular regions of the Pake pattern line shape away from the free ^{2}H frequency, thus increasing the splitting. The negative sign of the isotropic coupling is consistent with weak overlap of the p-orbital on C1 with the deuteron s-orbital.[63] The simulated ESEEM arising from the strong hyperfine coupling alone is shown in Figure 6A.

Simulation of the line shape also required a weak dipolar hyperfine coupling to reproduce the narrow central feature. The r_{eff} value for this hyperfine coupling was dependent upon the way in which the strong and weak ^{2}H hyperfine couplings were combined in the ESEEM simulations, as described in detail below. Individual ESEEM simulations for r_{eff} values of 3.3 and 3.8 Å, corresponding to two coupling combination models, are shown in Figure 6, B and C, respectively.

Comparison of the waveforms in Figure 6 shows that the amplitude of the modulation relative to the constant, or "dc",[44] amplitude is significantly larger for the shorter-range hyperfine coupling. Therefore, the $r_{eff} = 2.2$ Å coupling is expected to dominate the total ESEEM.

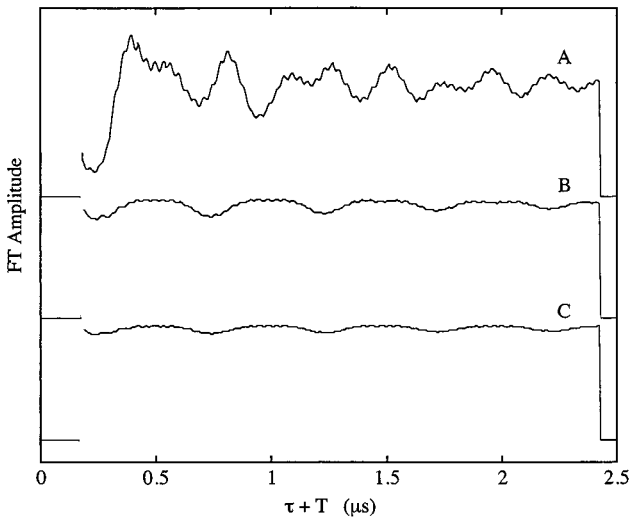

Figure 6. Quotient two-pulse ESEEM simulations for the (*S*)-2-aminopropanol-generated substrate radical in ethanolamine deaminase for individual hyperfine couplings. (A) Simulated quotient envelope modulation and frequency spectrum for $r_{eff} = 2.2$ Å and $A_{iso} = -0.35$ MHz. (B) Simulated quotient envelope modulation and frequency spectrum for $r_{eff} = 3.3$ Å and $A_{iso} = 0$. (C) Simulated quotient envelope modulation and frequency spectrum for $r_{eff} = 3.8$ Å and $A_{iso} = 0$. Fixed simulation parameters are described in Experimental Procedures.

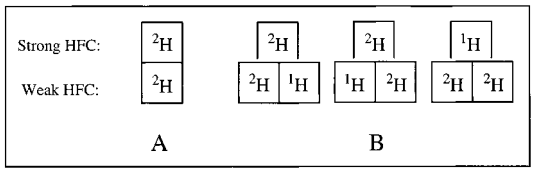

Figure 7. Schematic representation of the two models used for combination of the simulated ESEEM. Rows 1 and 2 represent the strong hyperfine coupling (HFC) and weak hyperfine coupling. (A) Simple model. The strongly and weakly coupled hydrogen nuclei are present in 1:1 proportion in a single population of enzyme active sites. (B) C5′ methyl group model. The strongly and weakly coupled hydrogen nuclei are present in 1:2 proportion, and the three active site populations reflect the permutations of occupancy of the three hydrogen sites by two ^{2}H and one ^{1}H.

Combination of the ^{2}H Hyperfine Couplings. The two-pulse ESEEM in the case of multiple hyperfine couplings (≥2 nuclei interacting with the same electronic wave function) is given by the product of the ESEEM from the individual hyperfine couplings,[43] as shown by eq 2. In the most simple model for the unpaired electron-^{2}H interactions, the electron is coupled to one strong and one weak ^{2}H in each enzyme active site, as depicted in Figure 7A. For this model, the total quotient ESEEM is the product of the quotient ESEEM from the strong and weak hyperfine couplings, as given by eq 6. Figure 8A shows the best simulated ESEEM for this simple model, which was obtained by using the strong hyperfine coupling and the $r_{eff} = 3.3$ Å weak dipolar coupling. The value of $r_{eff} = 3.3$ Å was found to give the correct relative amplitude of the central and broad features in the total ESEEM line shape. However, although the match to the line shape was good (comparable to the simulation shown in Figure 5), the amplitude of the envelope modulation in the time-domain simulation is more than double the experimental modulation amplitude. This indicates that the contributions of the strong and weak hyperfine coupling to the total ESEEM are not given by a direct product. Specifically, the contribution of the $r_{eff} = 2.2$ Å coupling to the total modulation requires attenuation. Additional assumptions about

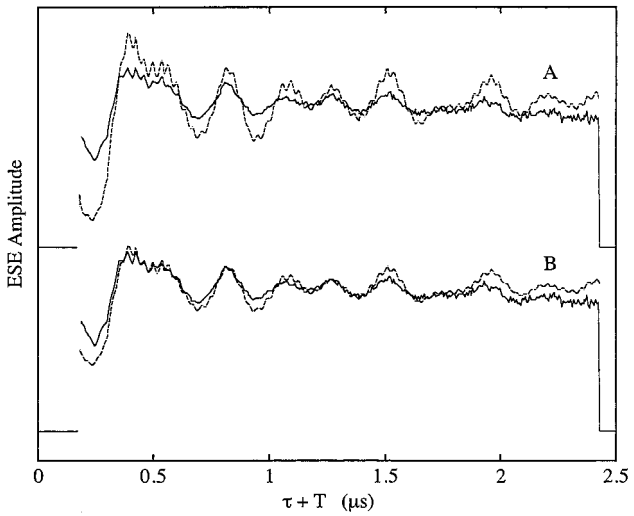

Figure 8. Experimental two-pulse quotient ESEEM (solid line) and overlaid quotient ESEEM simulations (dashed line). (A) ESEEM simulation for the simple coupling model, which is depicted in Figure 7A. (B) ESEEM simulation for the C5′ coupling model, which is depicted in Figure 7B. Conditions for the experimental ESEEM are given in Figure 4.

the electron−deuteron interactions in the active site of ethanolamine deaminase are required.

We consider a structural model where the coupled hydrogen nuclei are bonded to the C5′ methyl group. In the substrate radical state, C5′ is a methyl center in 5′-deoxyadenosine. After undergoing ^2H exchange during the $^2H_4$-aminoethanol prelabeling step, two ^2H are bonded to C5′ when the enzyme is in the resting state (intact coenzyme bound), as depicted in Figure 1. The other two valencies on C5′ are filled by bonding to C4′ and Co^{III}. Upon subsequent formation of the substrate radical by abstraction of a ^1H atom from the natural abundance 2-aminopropanol substrate, the C5′ methyl group incorporates the single abstracted ^1H nucleus, along with two ^2H nuclei. If reorientation of the methyl group occurs during the cryotrapping time of 15 s, which is likely, then the positions of the hydrogen sites relative to the unpaired electron spin localized at C1 of the substrate would be randomized with respect to ^2H or ^1H occupancy. Figure 7B depicts the three populations of enzyme active sites present in the sample.

ESEEM simulations performed under these assumptions converged to two equivalent weak hyperfine couplings (r_{eff} = 3.8 Å; uncertainty approximately ±0.1 Å), along with the single strong hyperfine coupling (r_{eff} = 2.2 Å, A_{iso} = −0.35 MHz). The resolution of the experimental data does not allow the two weak hyperfine couplings to be distinguished. The quotient ESEEM for the heterogeneous active site distribution is simulated by using eq 7, and is presented in Figure 8B. The match with the experimental envelope modulation amplitude is very good. Mismatch at 2.0−2.5 μs is caused by a slightly more rapid background decay of the envelope modulation in the ^2H sample. The time domain simulation in Figure 8B is successful because the contribution of active sites with two weakly coupled ^2H (proportionately, 0.33 of the total) carries relatively small envelope modulation amplitude, and therefore, a correspondingly large unmodulated, or "dc",[44] amplitude. This has the effect of attenuating the envelope modulation depth contribution of the r_{eff} = 2.2 Å coupling in the total ESEEM. The increase in r_{eff} from 3.3 to 3.8 Å is accompanied by a decrease in the envelope modulation depth, without a change in line width (full width at half-maximum, fwhm, is 0.31 MHz for both r_{eff} values). This is because the length of the time domain (3 μs) determines the fwhm [$\sim(3\ \mu s)^{-1}$ = 0.3 MHz] for $r_{eff} > 3.1$ Å.

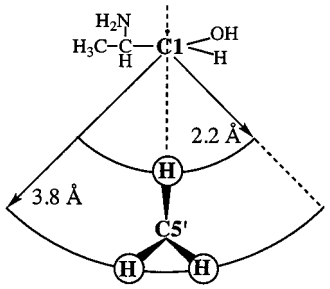

Figure 9. Model for structure of the C1 substrate radical and C5′-methyl group of 5′-deoxyadenosine in the active site of ethanolamine deaminase. The r_{eff} values, which are derived from the ESEEM analysis, are shown. With the strongly coupled H atom positioned at r_{eff} = 2.2 Å from C1, the weakly coupled H atoms of the C5′ methyl group lie on the r_{eff} = 3.8 Å surface when the C1−H_{strong}−C5′ bond angle is 159°. At the C1−C5′ distance of 3.2 Å, steric constraints from C1 substituents force C5′ to occupy a region below the trigonal plane of C1, as depicted in the Figure.

The Fourier transform of the simulation in Figure 8B is shown overlaid with the experimental spectrum in Figure 5. The simulated and experimental line shapes match well. The origin of the slightly diminished resolution of the experimental line shape (and corresponding more rapid damping of the envelope modulation) is not known. It may be caused by modest dispersion in the hyperfine coupling tensors, caused by a narrow static distribution[65] of electron−nuclear distances. On the basis of the success of this simulation analysis in reproducing both the envelope modulation amplitude and the ESEEM line shape, the coupled ^2H are assigned to sites on the C5′ methyl group of 5′-deoxyadenosine.

Consideration of Protein-Based Hydrogen Atom Exchange Sites. Amino acid-based radicals participate in hydrogen atom exchange reactions associated with radical-mediated catalysis in other enzyme systems.[5,66] These radical centers offer a single exchangeable hydrogen atom. In contrast, we observe at least two coupled hydrogen sites, and find that three coupled hydrogen sites (C5′ model) are required to match simulation and experiment. It is therefore difficult to rationalize the ESEEM results on the basis of a single exchangeable hydrogen site. The incorporation of a small, unquantitated amount of tritium into a putative protein site in ethanolamine deaminase during turnover[67] may result from a side-reaction, perhaps related to the inactivation phenomena observed in this[2,68] and other[5,66] enzymes that use electron-deficient radicals in catalysis.

Structure in the Active Site. Figure 9 presents a model for the substrate radical C1 interaction with the C5′ methyl group of 5′-deoxyadenosine in the active site of ethanolamine deaminase. The r_{eff} values are consistent with the methyl group structure (sp^3-hybridized carbon, r(CH) = 1.1 Å, r(HH) = 1.6 Å). With the strongly coupled hydrogen (H_{strong}) positioned 2.2 Å from C1, a distance to the two weakly coupled hydrogens of 3.8 Å is attained when the C1−H_{strong}−C5′ angle is 159°. Therefore, the C1−H_{strong}−C5′ angle is bent from the linear

(65) (a) Warncke, K.; McCracken, J. *J. Chem. Phys.* **1995**, *103*, 6829−6840. (b) Warncke, K.; Babcock, G. T.; McCracken, J. *J. Phys. Chem.* **1996**, *100*, 4654−4661.

(66) *Metalloenzymes Involving Amino Acid-Residue and Related Radicals*; Sigel, H., Sigel, A., Eds.; Marcel Dekker: New York, 1994; Vol. 30.

(67) O'Brien, R. J.; Fox, J. A.; Kopczynski, M. G.; Babior, B. M. *J. Biol. Chem.* **1985**, *260*, 16131−16136.

(68) Graves, S. W.; Fox, J. A.; Babior, B. M. *Biochemistry* **1980**, *19*, 3630−3630.

180° arrangement. If optimal hydrogen transfer is achieved when the C1−H_{strong}−C5′ centers are in-line, a bent arrangement suggests a structural deterrent to radical pair recombination.

The geometry of the model in Figure 8 leads to an estimation of 3.2 Å for the C1−C5′ separation distance.[69] We therefore conclude that C1 and C5′ are at closest contact. The uncertainty in this estimate, derived from the uncertainty in the r_{eff} value obtained from simulation of the ^{2}H sum combination line position, is <0.1 Å. In a ^{13}C pulsed-ENDOR study of the substrate radical state that employed adenosylcobalamin labeled with ^{13}C at all five ribosyl carbon positions, the point dipole distance between the unpaired electron and a ^{13}C nucleus, assigned to C5′, was determined to be 3.4 ± 0.2 Å.[18] This is the same as our estimation of the C1−C5′ distance within error.

(69) The C1−C5′ distance of 3.2 Å is a lower limit, because it is derived from values for r_{eff}, which are obtained by using the point dipole approximation for the C1−^{2}H interaction. Accounting for the spatial extent of the p-orbital on C1 that contains the unpaired electron would be expected to cause a lengthening of the electron−^{2}H distance, but probably by no more than a few tenths of an angstrom. This would extend the C1−C5′ distance by a corresponding amount.

Radical Migration and the Mechanism of Catalysis. The close proximity of C1 and C5′ in the substrate radical state indicates that the 5′-deoxyadenosyl radical directly abstracts hydrogen from the substrate. Further, we propose that the C5′ methyl group is the direct hydrogen atom donor to the product radical, because of its poising in the substrate radical state, near to the C2 carbon center where this exchange occurs in the product radical state. Thus, hydrogen atom exchanges with the substrate and product species are proposed to be directly mediated by the 5′-deoxyadenosyl radical/5′-deoxyadenosine couple. This reaction path corresponds to Path 1 of Figure 1. In combination with the ∼10−12 Å distance between Co^{II} and C1,[62] and a Co−C5′ bond length of 1.97 Å,[8] our results indicate that C5′ undergoes a displacement of 5−7 Å during radical pair separation in ethanolamine deaminase.

Acknowledgment. Supported by Grant R01 DK54514 from the National Institutes of Health. We thank Ms. Lori Anderson for technical assistance and Professor Dale E. Edmondson (Emory University) for use of fermentation facilities.

JA003658L